miR-130b/301b Is a Negative Regulator of Beige Adipogenesis and Energy Metabolism In Vitro and In Vivo

Wenyi Luo,[1,2] Youngsil Kim,[1] Mary Ellen Jensen,[1] Oana Herlea-Pana,[3] Weidong Wang,[1,3] Michael C. Rudolph,[1,4] Jacob E. Friedman,[1,4] Steven D. Chernausek,[1,5] and Shaoning Jiang[1,5]

Diabetes 2022;71:2360–2371 | https://doi.org/10.2337/db22-0205

Thermogenic brown or beige adipocytes dissipate energy in the form of heat and thereby counteract obesity and related metabolic complications. The miRNA cluster miR-130b/301b is highly expressed in adipose tissues and has been implicated in metabolic diseases as a post-transcriptional regulator of mitochondrial biogenesis and lipid metabolism. We investigated the roles of miR-130b/301b in regulating beige adipogenesis in vivo and in vitro. miR-130b/301b declined in adipose progenitor cells during beige adipogenesis, while forced overexpression of miR-130b-3p or miR-301b-3p suppressed uncoupling protein 1 (UCP1) and mitochondrial respiration, suggesting that a decline in miR-130b-3p or miR-301b-3p is required for adipocyte precursors to develop the beige phenotype. Mechanistically, miR-130b/301b directly targeted AMP-activated protein kinase (AMPKα1) and suppressed peroxisome proliferator–activated receptor γ coactivator-1α (*Pgc-1α*), key regulators of brown adipogenesis and mitochondrial biogenesis. Mice lacking the miR-130b/301b miRNA cluster showed reduced visceral adiposity and less weight gain. miR-130b/301b null mice exhibited improved glucose tolerance, increased UCP1 and AMPK activation in subcutaneous fat (inguinal white adipose tissue [iWAT]), and increased response to cold-induced energy expenditure. Together, these data identify the miR-130b/301b cluster as a new regulator that suppresses beige adipogenesis involving PGC-1α and AMPK signaling in iWAT and is therefore a potential therapeutic target against obesity and related metabolic disorders.

Obesity results from long-term imbalances between energy intake and energy expenditure (EE) and is a global health problem that increases the risk of diabetes, cardiovascular disease, nonalcoholic fatty liver disease, and certain cancers (1). White adipose tissues (WAT) are located in multiple subcutaneous and visceral locations in the body and serve as the main sites of lipid storage. In comparison, brown adipose tissue (BAT) is responsible for thermogenic EE and contributes to triglyceride clearance and glucose homeostasis (2). In addition to classical brown adipocytes, thermogenic adipocytes reside within WAT depots and are referred to as beige or BRITE cells. These cells show morphology and thermogenic function similar to those of brown adipocytes: they have numerous mitochondria and express brown fat-specific uncoupling protein 1 (UCP1), which uncouples oxidative respiration to generate heat and dissipate energy (3). Numerous studies in rodents and humans have demonstrated that the activity and development of brown and beige adipose tissues are inhibited in obesity and diabetes (4,5) and that "browning" of WAT (beige adipogenesis) is protective against obesity (6). With the recent discovery of active BAT/beige depots in adult humans (7), strategies targeting key elements controlling the formation of brown

[1]Harold Hamm Diabetes Center, University of Oklahoma Health Sciences Center, Oklahoma City, OK
[2]Department of Pathology, University of Oklahoma Health Sciences Center, Oklahoma City, OK
[3]Department of Medicine, University of Oklahoma Health Sciences Center, Oklahoma City, OK
[4]Department of Physiology, University of Oklahoma Health Sciences Center, Oklahoma City, OK
[5]Section of Diabetes and Endocrinology, Department of Pediatrics, University of Oklahoma Health Sciences Center, Oklahoma City, OK

Corresponding author: Shaoning Jiang, shaoning-jiang@ouhsc.edu

Received 27 February 2022 and accepted 22 August 2022

This article contains supplementary material online at https://doi.org/10.2337/figshare.20536392.

and beige adipocytes hold promise to combat obesity in humans.

WAT and beige adipocytes arise from a common pool of adipose progenitor cells, but the control of this process at a molecular level is incompletely understood. The differentiation and development of brown and beige adipocytes are regulated by numerous transcription factors and hormones, operating via signaling pathways that promote mitochondrial biogenesis and UCP1 expression (8,9). miRNAs are small noncoding RNAs that can have dramatic effects on cell development and function by regulating post-transcriptional gene expression involving multiple targets (10–12). miR-130b and miR-301b are two closely related miRNAs that are adjacent in the genome and share a common promoter and seed sequence. miR-130b and miR-301b are of particular interest as they have been linked to abnormal blood lipid levels in genome-wide association studies involving >188,000 individuals (13) and were recently found to predict weight gain over a 5-year period in adult women (14). These data suggest involvement of these miRNAs in fat metabolism, yet the function of miR-130b/301b outside of oncogenesis remains poorly understood (15,16). Our published human studies have shown that human miR-130b expression is upregulated in adipocytes and macrophages of young adults with obesity (17), as well as in umbilical vein endothelial cells from offspring born to women with diabetes (18). Direct targets of miR-130b-3p and miR-301b-3p include AMP-activated protein kinase (AMPKα) (19) and peroxisome proliferator–activated receptor γ coactivator-1α (PGC-1α) (20,21), key regulators of brown/beige adipogenesis and function (22–24). However, the roles of miR-130b/301b in beiging and whole-body metabolism remain unexplored. Given the strong link of miR-130b/301b to metabolic health and AMPK/PGC-1α in energy metabolism, we focused on defining the specific roles of miR-130b/301b in the control of beige adipocyte formation, in vitro, and for the first time in null mutant mice.

RESEARCH DESIGN AND METHODS

Murine Studies

The miR-130b/301b loxP-flanked (loxp sites flanking the miR-130b and miR-301b region) mice (no. 034655) and CMV-Cre mice (25) (no. 006054) were purchased from The Jackson Laboratory. The mice were backcrossed to the C57BL/6J background for >10 generations. Homozygous miR-130b/301b fl/fl mice were bred with CMV-Cre mice to produce miRNA-130b/301b heterozygous progeny. Male and female heterozygous mice were crossed to produce homozygous knockouts (KO) and wild-type (WT) control littermates. The homozygous KO were identified by genotyping using primers: 5′CCTCACCTACTGTTCCTTCTTTC3′ (forward) and 5′TGGCTGGAGTGGGATCTTA3′ (reverse). Only male offspring and cells were studied, as males are more susceptible to high-fat diet (HFD)-induced obesity (26). After weaning, male WT and KO littermates (5–6 weeks of age) were fed an HFD (D12451; Research Diets) with 45% energy from fat or a chow control diet (10% of kilocalories from fat, D12450Hi; Research Diets). Mice were housed at room temperature (21°C) under a 12-h light/dark cycle (from 6:00 A.M. to 6:00 P.M.), with ad libitum access to diet and water. Body weights were monitored weekly, and body composition (total fat and lean mass) was measured with quantitative magnetic resonance (EchoMRI Whole Body Composition Analyzer; Echo Medical Systems). At the end of the experiments, mice were euthanized and freshly dissected tissues flash-frozen in liquid N_2 and stored at −80°C or fixed in 4% paraformaldehyde for histology. Inguinal WAT (iWAT), BAT, and visceral fat depots (including epididymal WAT [eWAT], mesenteric, and perirenal depots) were dissected and weight was measured. All protocols for mice studies were approved by the University of Oklahoma Animal Care and Use Committee.

Indirect Calorimetry Measurements

Following 10 weeks of HFD feeding, the mice were placed in metabolic cages for measurement of metabolic activities at room temperature (21°C) (Sable Systems, Las Vegas, NV), followed by measurement at thermoneutrality (28°C) (inside an environmental cabinet [Sable Systems]) a week later. For both the calorimetry measurements (21°C and 28°C), the mice were individually housed in the chambers and respiratory gas exchange was measured consecutively. The EE over 3 days was calculated with use of a modified Weir equation (EE [kilocalories per hour] = $60 \times [0.003941 \times VO_2 + 0.001106 \times VCO_2]$) (27).

Primary Adipose Progenitor Cell Culture and Differentiation

Stromal vascular fraction (SVF) cells were cultured as a source of primary adipose progenitor cells. SVF cells were isolated from iWAT of weaning mice as previously described with modification (22). Briefly, the inguinal adipose tissues were dissected and cut into small pieces with sterile scissors, followed by digestion with collagenase solution (1 mg/mL, 5 mL collagenase/gram of tissue) for 60 min at 37°C with shaking. After digestion, the solution and tissues were filtered through a sterile 70-μm cell strainer into a sterile 50-mL conical tube. The tubes were centrifuged at 450*g* at room temperature for 5 min. The SVF appeared as the dark red cells pelleted on the bottom. Red blood cells were lysed in ammonium-chloride-potassium red cell lysis buffer. The pelleted cells were resuspended and cultured in DME/F:12 medium with 15% FBS. After initial culture for 5 days nonadherent cells were intensively washed out and the adherent cells formed a cell population of progenitor cells (termed progenitor cells) (28), and beige adipogenesis was induced with a medium containing DMEM (GlutaMAX), 15% FBS, 1 μg/mL insulin, 1 μmol/L dexamethasone, 0.5 mmol/L

isobutyl-1-methylxanthine, 125 nmol/L indomethacin, and 1 nmol/L T3. After 3 days in induction medium, the medium was changed to maintenance medium containing 10% FBS, 1 μg/mL insulin, and 1 nmol/L T3. For white adipocyte differentiation the progenitor cells were induced with a medium containing DMEM (GlutaMAX), 15% FBS, 1 μg/mL insulin, 1 μmol/L dexamethasone, and 0.5 mmol/L isobutyl-1-methylxanthine for 3 days, and the medium was changed to maintenance medium containing 10% FBS and 1 μg/mL insulin. For β-agonists treatment, at 6 days after the induction of beige differentiation, the cells were treated with β-agonist isoproterenol (iso) (1 μmol/L) for 6 h or β-agonist CL316243 (CL) (1 μmol/L) for 20 h.

Transfection of miRNA Mimics

The primary progenitor cells were transfected with the miRNA mimics of miR-130b-3p (50 nmol/L) and miR-301b-3p (50 nmol/L) or the same amounts of a scrambled negative control miRNA using Lipofectamine RNAiMAX Transfection Reagent (0.25 μL RNAiMAX/100 μL medium, Life Technologies, Grand Island, NY) following the manufacturer's protocol. Efficiency of transfection was verified by fluorescent imaging and real-time PCR. In selected experiments, a mock control (Lipofectamine RNAiMAX Transfection Reagent only) group was included, which showed results similar to those of the transfection with the scrambled negative control (Supplementary Fig. 3*B*). The potential cytotoxicity of miRNA mimic transfection was evaluated in progenitor cells after transfection for 2 days with the MTT assay (Roche, Burlington, MA) according to manufacturer's protocol with absorbance measured at 550 nm with a reference wavelength of 690 nm.

Statistical Analysis

Normality was tested with the Kolmogorov-Smirnov test. For nonnormal data, Mann-Whitney *U* test was used to compare the differences between two groups. For data with normal distribution, differences between two groups were assessed with Student *t* test (two tailed, for in vitro studies). The statistical differences were analyzed with ANOVA for comparison among multiple groups. For comparison between the WT and KO mice littermates, Student paired *t* test (one tailed) was used. Software Excel was used for data analyses and bar graph plotting. P values <0.05 were treated as statistically significant. Additional methods can be found in Supplementary Material.

Data and Resource Availability

The data sets generated during or analyzed during the current study are available from the corresponding author on reasonable request. The mice generated during the current study are available from the corresponding author upon reasonable request.

RESULTS

Tissue-Specific Expression of miR-130b in iWAT Declines With Beige Adipogenesis

Analysis of selected tissues in the mouse showed that miR-130b was particularly abundant in iWAT as compared with other metabolically active tissues, including eWAT and BAT (Fig. 1*A*). SVF cells isolated from iWAT of WT mice were used for induction of beige adipogenesis or white adipogenesis in vitro as described (22,29,30). Following beige differentiation, the expression of miR-130b in iWAT progenitor cells started to decrease at 2 days and continued to decrease at 4 and 6 days (Fig. 1*B*), concordant with increases in the expression of thermogenic markers including *Ucp1*, *Pgc-1α*, and *Prdm16* (Fig. 1*C*). Expression of miR-130b also decreased in progenitor cells from eWAT and BAT (Supplementary Fig. 1) in response to beige differentiation but to a lesser extent. Following white adipogenic differentiation of iWAT progenitor cells, miR-130b expression did not decrease until 6 days after differentiation (Fig. 1*B*). In contrast to beige differentiation, induction of white adipogenesis only resulted in a slight increase in *Ucp1* expression (Fig. 1*C*). White adipogenic induction also increased expression of *Prdm16* (Fig. 1*D*) and *Pgc-1α* (Fig. 1*E*) but to a lesser extent at early stages of differentiation compared with beige adipogenic induction. Consistently, beige adipogenic differentiation of iWAT progenitors increased UCP1 protein abundance, which was further increased in response to β-agonists, including isoproterenol and CL316243 treatment (Fig. 1*F*).

miR-130b/301b Suppresses Beige Adipogenesis

For testing of whether a decline in miR-130b-3p and miR-301b-3p was necessary for beige adipogenesis, iWAT progenitor cells were transfected with miR-130b-3p, miR-301b-3p mimics, or scrambled controls. Beige adipogenesis was induced 2 days after transfection. Efficient and prolonged miR-130b-3p overexpression throughout the process of differentiation was achieved as evidenced by detection of red fluorescence in all the cells (Supplementary Fig. 2*A*) and significant increases in miR-130b-3p 8 days after transfection (Supplementary Fig. 2*B*). No cytotoxicity was observed with transfection of miR-130b or miR-301b mimics as determined by MTT assay (Supplementary Fig. 3*A*). miR-130b-3p or miR-301b-3p overexpression in adipose progenitor cells significantly reduced the formation of lipid droplets in response to beige differentiation (Fig. 2*A*). Overexpression of miR-130b-3p or miR-301b-3p also resulted in significant decreases in the abundance of UCP-1 protein (Fig. 2*B*) and mRNA (Fig. 2*C*). Expression of mitochondrial marker *Cox8a* was significantly decreased by miR-301b only (Fig. 2*C*), whereas a significant decrease in *Pgc-1α* mRNA (Fig. 2*C*) was observed only with overexpression of miR-130b-3p. Also, overexpression of miR-130b in adipose progenitor cells significantly decreased the expression of *PPARγ2* upon beige differentiation, whereas miR-301b resulted in increased *PPARγ2* expression (Fig. 2*C*).

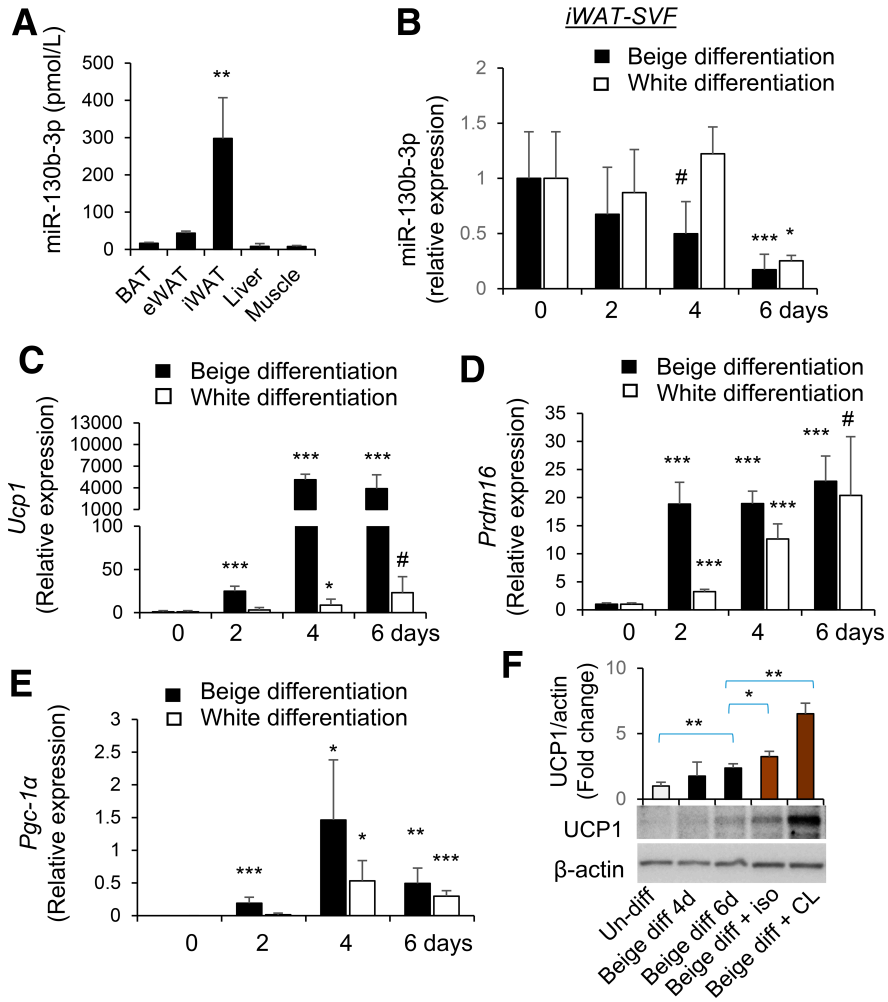

Figure 1—miR-130b tissue distribution and expression following beige and white adipogenic differentiation of isolated adipose progenitor cells. *A*: Levels of miR-130b-3p in BAT, eWAT, iWAT, liver, and muscle tissues of mice (normal diet, male, 6 weeks old) are shown. Mean ± SD, $N = 3$. *B–E:* SVF cells were isolated from iWAT from WT mice at the time of weaning followed by induction of beige or white adipogenesis in vitro. At 0, 2, 4, and 6 days after differentiation, fold changes of mRNA levels of miR-130b-3p (*B*) and *Ucp1* (*C*), *Prdm16* (*D*), and *Pgc-1α* (*E*) in undifferentiated and beige or white adipogenic (adipo-) differentiated adipocytes from iWAT were measured by real-time PCR and normalized to Sno234 (*B*) or TBP (TATA box binding protein gene) (*C–E*). $n = 3$–7 in each group, mean ± SD. *$P < 0.05$, **$P < 0.01$, ***$P < 0.001$, #$P < 0.05$ (one tail) compared with day 0 undifferentiated cells. *F*: After 6 days of beige differentiation (diff), the cells were treated with β-agonists isoproterenol (iso) (1 μmol/L) for 6 h or CL316243 (CL) (1 μmol/L) for 20 h. Representative blots showing protein levels of UCP1, $n = 3$–4/group. d, days; Un-diff, undifferentiated.

No effect of miR-130b or miR-301b on *Perilipin A* expression was observed (Fig. 2*C*). Despite the discrepancy, both miR-130b and miR-301b significantly decreased levels of *Adiponectin* (Fig. 2*C*), as well as the thermogenic regulator type 2 deiodinase (*Dio2*) (Fig. 2*C*). These data demonstrate that miR-130b and miR-301b have the capacity to inhibit beige adipogenic differentiation, with potential differences between miR-130b and miR-301b.

miR-130b/301b Suppresses Mitochondrial Respiration in Progenitor Cells After Induction of Beige Adipogenic Differentiation

To address the functional properties of the differentiated beige adipocytes, we examined bioenergetic kinetics using the Seahorse extracellular analyzer (Agilent Seahorse). Overexpression of miR-130b-3p or miR-301b-3p in progenitor cells led to a decrease in the basal oxygen consumption rates (OCR) and OCRs for proton leak following induction of beige adipocyte differentiation (Fig. 3). Maximal respiration was also significantly suppressed by miR-130b overexpression only (Fig. 3). These data demonstrate that adipose progenitor cells differentiated in the presence of increased miR-130b/301b exhibit decreased mitochondrial respiration, an important functional characteristic of beige adipocytes. To determine the direct impact of the miR-130b on mitochondrial genes, we transfected differentiated mature beige adipocytes with miR-130b-3p mimics and analyzed markers of beiging genes at 2 days after transfection. As the results show in Supplementary Fig. 4, miR-130b overexpression had no significant impact

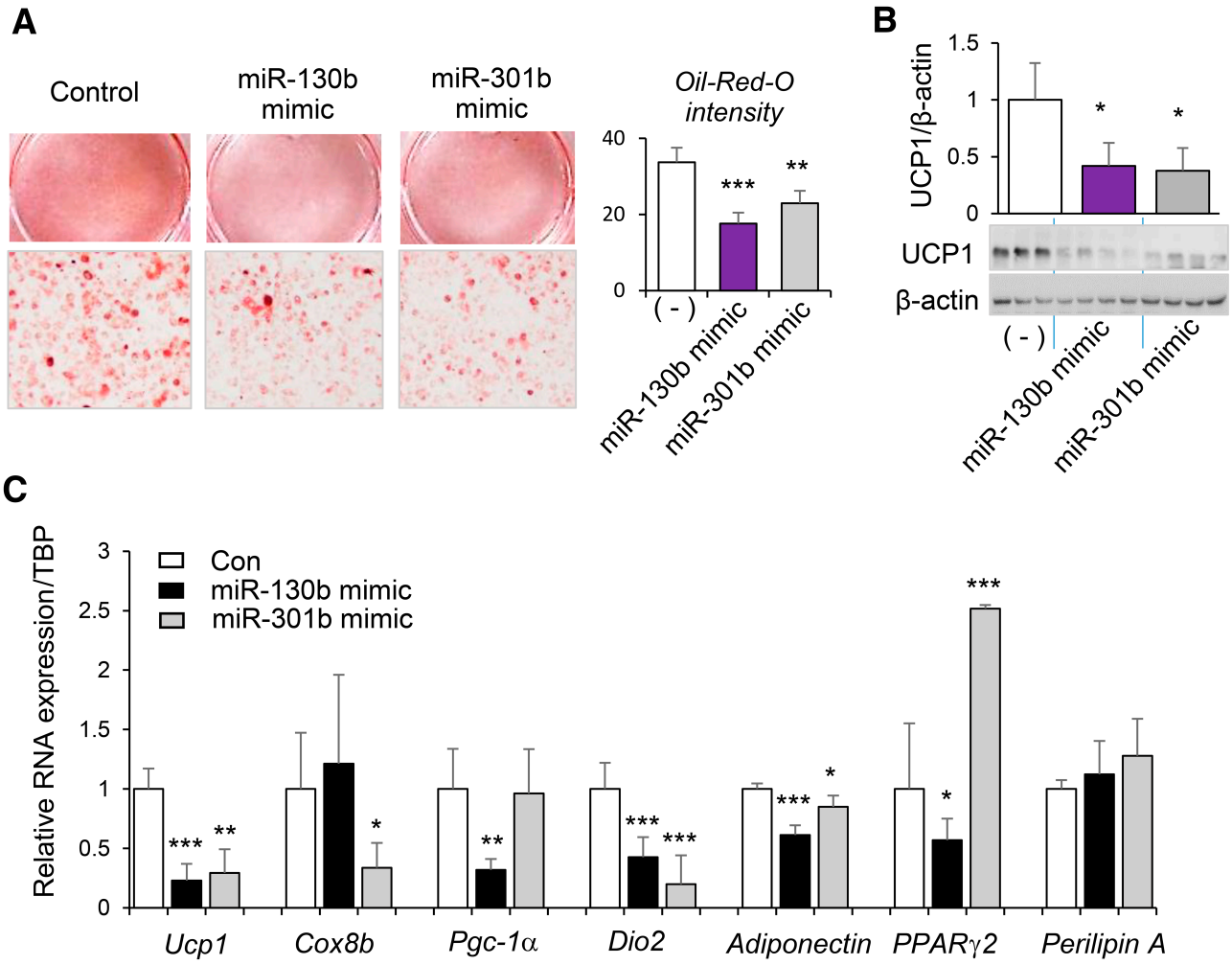

Figure 2—Role of miR-130b/301b in beige adipogenic differentiation of progenitor cells isolated from fat tissue. SVF cells were isolated from iWAT from WT mice at the time of weaning and transfected with miR-130b-3p mimics, miR-301-3p mimics, or negative control. Beige adipogenic differentiation was induced at 2 days after transfection. At 6 days after differentiation, oil red O staining of beige differentiated cells (*A*), protein abundance of UCP1 (*B*), and *Ucp1*, *Cox8a*, *Pgc-1α*, *Dio2*, *Adiponectin*, *PPARγ2*, and *Perilipin A* mRNAs (*C*) are shown. Con, control. Mean ± SD, $n = 3$–4 in each group. *$P < 0.05$, **$P < 0.01$, ***$P < 0.001$ compared with negative control (–).

on expression of mitochondrial genes, including *Ucp1*, *Cox8a*, and *Pgc-1α*, in mature beige adipocytes. Therefore, miR-130b likely acts on progenitor cells to impair their capacity to differentiate to beige adipocytes, and the effects on mitochondria respiration after beige adipogenic induction are likely due to decreased beige adipogenic differentiation.

miR-130b/301b Reduces AMPKα1 Expression

miR-130b/301b is reported to directly target the 3′-untranslated region (3′-UTR) of AMPKα1 (19). Concomitant with increased expression of thermogenic markers as shown in Fig. 1*C*–*E*, AMPK signaling was activated upon beige differentiation of progenitors, evidenced by significant increase in phosphorylation of ACC (P-ACC) (Fig. 4*A*). In the iWAT adipose progenitor cells, overexpression of miR-130b-3p and miR-301b-3p resulted in decreased abundance of AMPKα1 protein (Fig. 4*B*). Similarly, following induction of brown differentiation, abundance of AMPKα1 and downstream P-ACC were significantly decreased by overexpression of miR-130b-3p and miR-301b-3p (Fig. 4*C*). The capacity of miR-130b and miR-301b to directly suppress the 3′-UTR of AMPK (Fig. 4*D*) was further demonstrated by the significant suppression of the luciferase reporter activity by miR-130b and miR-301b (Fig. 4*E*).

The effects of miR-130b and miR-301b during white adipogenesis of iWAT progenitors were assessed. White adipogenic induction significantly increased P-ACC (Supplementary Fig. 5*A*). Despite decreased AMPK activation (P-ACC) (Supplementary Fig. 5*B*) and suppression of adiponectin mRNA expression by miR-130b mimics (Supplementary Fig. 5*C*), white adipogenic markers including *Fabp4* and *C/EBPα* were not altered by miR-130b or miR-301b overexpression, whereas type 2 deiodinase (Dio2), a transcriptional regulator of thermogenic genes (31), was significantly suppressed by miR-130b and miR-301b (Supplementary

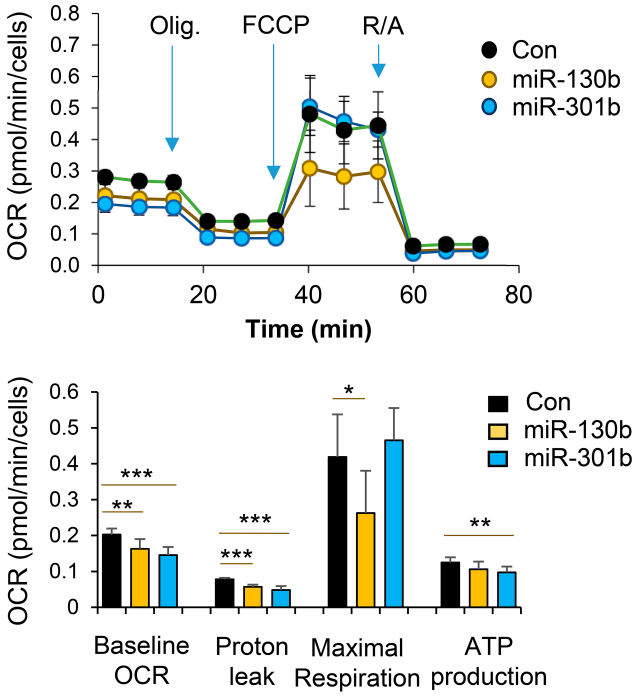

Figure 3—Role of miR-130b/301b in mitochondrial respiration in beige adipogenic differentiated progenitor cells isolated from fat tissues. SVF cells were isolated from iWAT from WT mice at the time of weaning. The progenitor cells were transfected with miR-130b-3p mimics, miR-301-3p mimics, or negative control (Con). Beige adipogenic differentiation was induced at 2 days after transfection. At 3 days following beige differentiation, OCR was measured over time and after stress treatment of Oligomycin (Oligo, 1 μmol/L), FCCP (1 μmol/L), and rotenone and antimycin A (R/A) (0.5 μmol/L). Indices of baseline OCR, proton leak, maximal respiration, and ATP production were calculated according to altered OCR following the treatment. Mean ± SD, $n = 8$ in each group. *$P < 0.05$; **$P < 0.01$; ***$P < 0.001$.

Fig. 5*C*). These results suggest that miR-130b/301b are not likely involved in white adipogenesis, at least in progenitors from subcutaneous fat depot.

Mice Lacking miR-130b/301b Have Reduced Visceral Fat and Improved Glucose Tolerance

Mice deficient in both miR-130b and miR-301b and the WT littermates were produced by crossing of the male and female miR-130b/301b heterozygous mice. Homozygous null mutants were identified by the absence of miR130b/301b gene cluster and lack of miRNA expression (data not shown). The miR-130b/301b null mice (miR-130b/301b$^{-/-}$) were viable and fertile with no obvious physical or behavioral abnormalities. The miR-130b/301b$^{-/-}$ mice gained less weight compared with WT littermates following a chow diet or 12 weeks on an HFD (Fig. 5*A*). The miR-130b/301b$^{-/-}$ mice tended to have less total body fat, but not lean mass, as measured with EchoMRI (Fig. 5*B*). The percentage of visceral fat weight, but not iWAT nor BAT, of miR-130b/301b$^{-/-}$ mice was significantly lower compared with that of the WT littermates after HFD or chow diet (Fig. 5*C*). In addition, the miR-130b/301b$^{-/-}$ mice displayed modestly improved glucose tolerance after HFD (Fig. 5*D*). Fasting blood insulin concentration and insulin sensitivity index measured with HOMA of insulin resistance were not significantly different between KO and WT mice (Fig. 5*E*).

miR-130b/301b KO Mice Have Increased Beiging of Subcutaneous iWAT Fat Depots and Increased Capacity of Cold-Induced EE

Histologic examination of the brown fat (BAT), the eWAT, and subcutaneous WAT (iWAT) in miR-130b/301b KO mice following 12 weeks on HFD revealed smaller adipocyte size and lipid droplets in iWAT compared with WT littermates (Fig. 6*A*). There were no significant histological differences in BAT or eWAT between the KO mice and WT littermates (Fig. 6*A*). Histological staining in iWAT for UCP1 showed that the smaller cells were positive for UCP1 expression (Fig. 6*B*). Expression of UCP1 was significantly higher in iWAT of miR-130b/301b KO mice compared with WT littermates (Fig. 6*C*), consistent with the "beige-ing" of subcutaneous fat. PGC-1α protein was higher in iWAT of the miR-130b/301b KO mice (approaching significance $P = 0.07$) (Fig. 6*D*). In addition, ablation of miR-130b/301b resulted in increased AMPKα and P-ACC in iWAT of HFD-fed mice compared with WT mice (Fig. 6*D*), indicating activation of AMPK signaling. Consistently, mRNA expression of thermogenic markers, including *Prdm16*, *Cox8b* and *Pgc-1α*, was significantly higher in iWAT of miR-130b/301b KO mice (Fig. 6*E*).

For evaluation of the influence of miR-130b/301b on whole-body energy homeostasis, EE was measured following 10 weeks of an HFD at room temperature (21°C) and at thermoneutrality (28°C), the temperature zone within which there is almost no thermogenesis or heat production (32). WT and KO mice displayed equivalent EE at thermoneutrality 28°C, but KO mice tended to have greater EE at 21°C ($P = 0.08$) during the dark cycle (Fig. 6*F*). The net increase between 28°C and 21°C was to a significantly greater extent in KO mice during both dark and light cycles (Fig. 6*F*), suggesting increased capacity for thermogenic EE in response to cold stimulation.

DISCUSSION

Prior studies by our group (17,18) and others (13,20) have revealed that the expression of miR-130b and miR-301b is increased in human metabolic disorders, such as obesity, dyslipidemia, and gestational diabetes mellitus, as well as in animal models of obesity (19,20). In the current study, combining in vitro and in vivo approaches using primary adipose progenitor cells and genetically modified mice, we show that miRs-130b/301b are important determinants of beige adipocyte development and function.

The capacity of WAT progenitors to form mature, beige adipocytes declines in obesity and diabetes (33,34). Our studies of progenitor cells cultured from iWAT demonstrate an inhibitory role for miR-130b/301b in beige

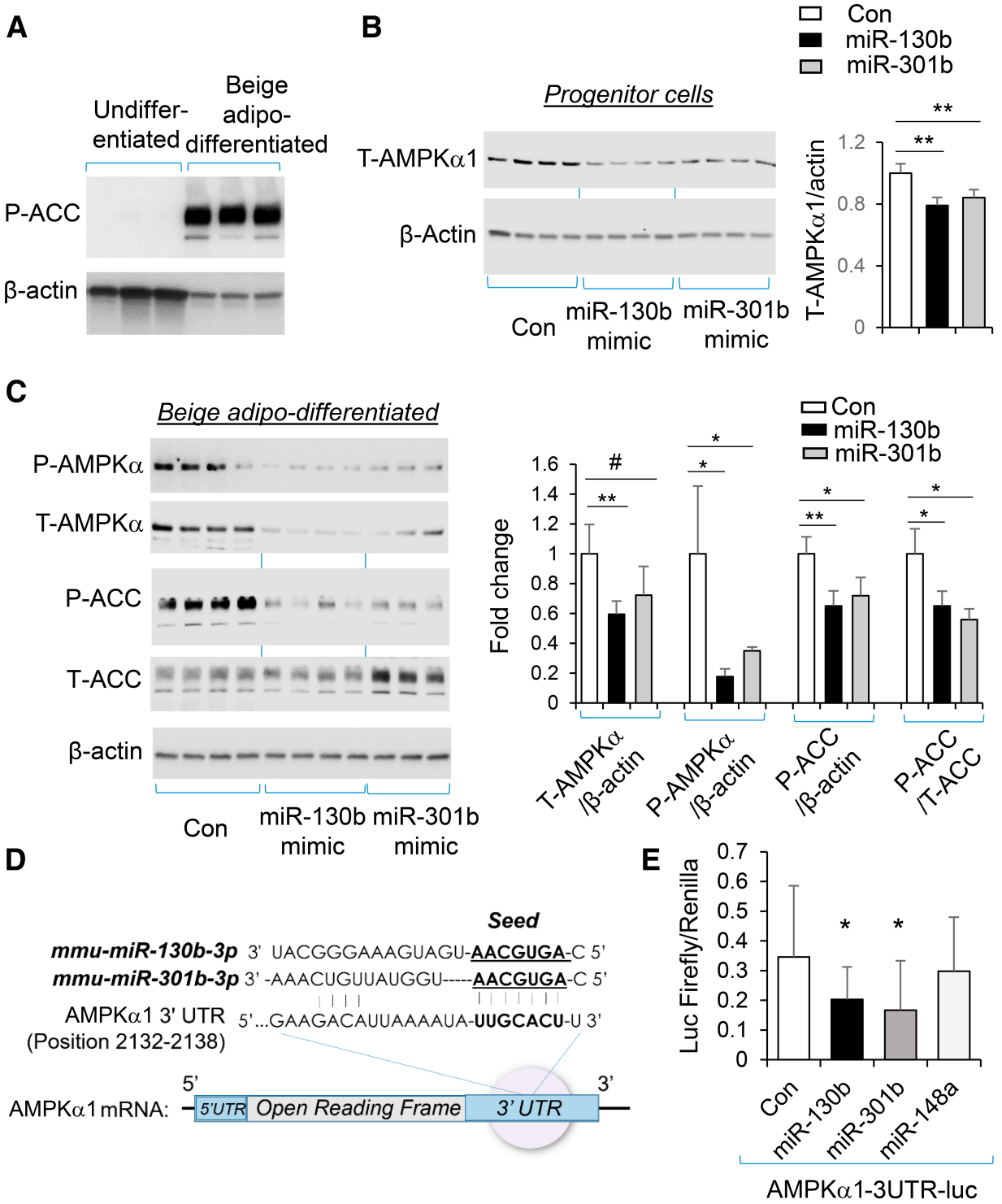

Figure 4—miR-130b/301b targets AMPKα expression in adipose progenitors from iWAT. SVF cells were isolated from inguinal white fat from WT mice at the time of weaning. *A*: Level of P-ACC following beige adipogenic (adipo-) differentiation (6 days). *B*: The progenitor cells from iWAT of mice were transfected with miR-130b-3p mimics, miR-301b-3p mimics, or negative control (Con). Total (T-)AMPKα protein level was measured at 2 days after transfection. *C*: Beige adipogenic differentiation was induced at 2 days after transfection of miR-130b-3p mimics, miR-301b-3p mimics, or negative control. At 3 days following beige differentiation, total AMPKα and P-ACC (S79) levels were shown. $N = 3$–4. $^*P < 0.05$; $^{**}P < 0.01$. $P < 0.05$ by one-tail *t* test. *D*: Diagram of AMPKα1 3′-UTR sequence targeted by miR-130b-3p and miR-301b-3p. *E*: The iWAT progenitors were cotransfected with luciferase reporter plasmid containing the AMPK 3′-UTR (position 1728–2226 [includes the miRNA binding sites]), with mimics of miR-130b-3p, miR-301b-3p, or miR-148a-3p. After 48 h, the firefly/Renilla luciferase (Luc) activity was measured. Mean ± SD, $n = 9$–12 in each group. Same results were confirmed in repeated experiments. $^*P < 0.05$.

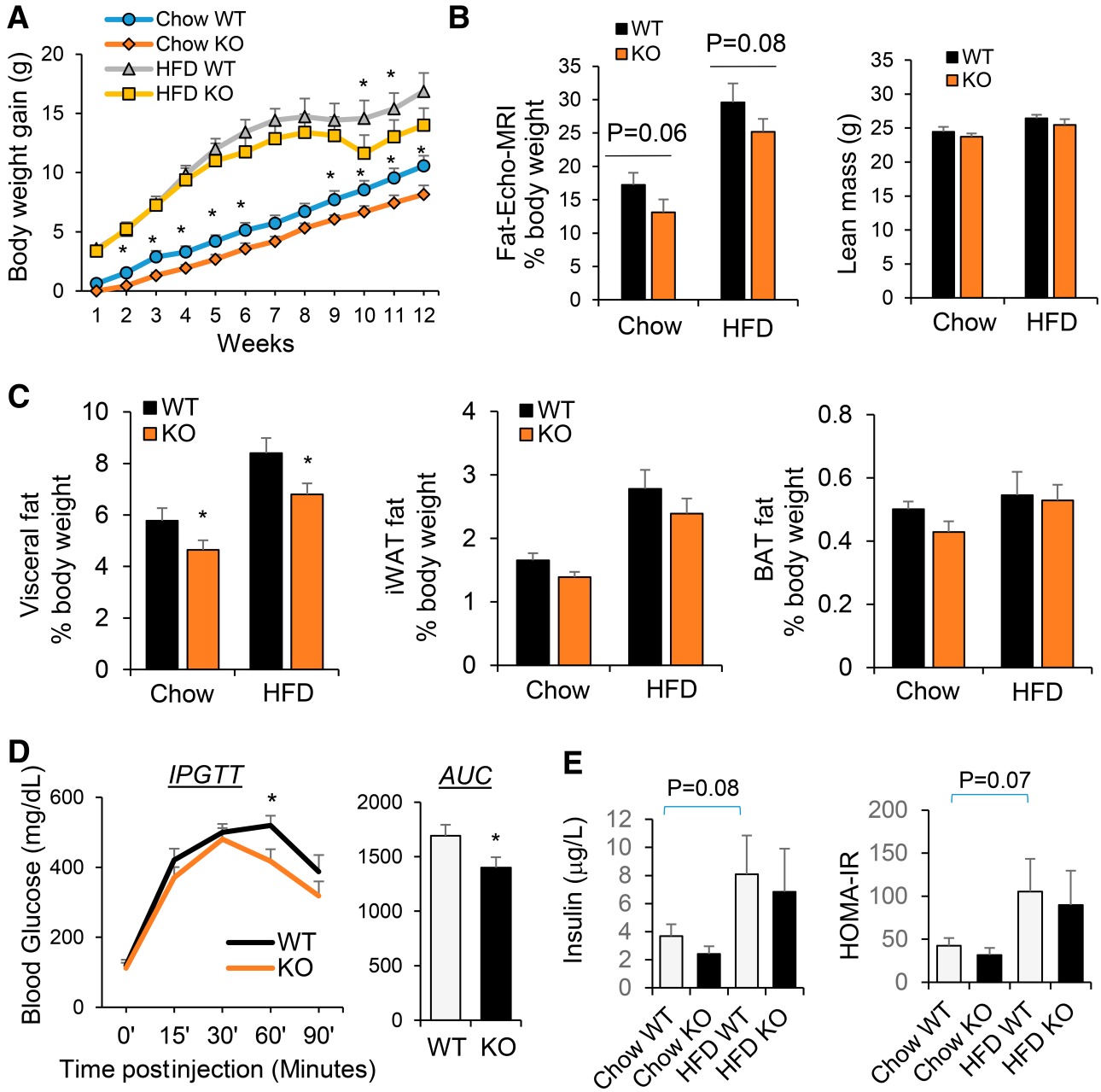

Figure 5—Metabolic characterization of miR-130b/301b KO mice following chow or HFD. miR-130b/301b KO and WT littermates (males) were fed with HFD (45% kcal fat, 20% kcal protein, 35% kcal carbohydrate) or control diet (chow) at 5–6 week-old age. *A*: Weekly body weight gain following HFD or chow feeding. *B*: Total body fat and lean mass of mice following HFD or chow diet for 12 weeks were measured with EchoMRI, and fat mass was normalized to body weight. *C*: The visceral fat, iWAT, and BAT fat mass percentage of body weight after HFD or chow feeding. *D*: Glucose tolerance testing was performed after HFD for 10 weeks. Blood glucose levels during the glucose tolerance test and the area under the curve are shown. AUC, area under the curve; IPGTT, intraperitoneal glucose tolerance test. *E*: Insulin levels and glucose levels in the serum of the mice after 4 h fasting were measured. Insulin sensitivity index was calculated based on the following equation: HOMA of insulin resistance (HOMA-IR) = (fasting plasma insulin × fasting plasma glucose) / 22.5. Mean ± SEM, $n = 7$ WT-KO littermates pairs. *$P < 0.05$.

adipogenesis, particularly in the subcutaneous iWAT depot. miR-130b-3p expression declined during beige adipocyte differentiation, and also forced overexpression of miR-130b-3p or miR-301b-3p in iWAT progenitor cells decreased the abundance of thermogenic *Ucp1* and *Dio2* expression, lipid formation, adiponectin, and mitochondrial respiration. Despite decreased miR-130b-3p following white adipocyte differentiation, overexpression of miR-130b-3p or miR-301b-3p in iWAT progenitor cells did not alter white adipogenic markers including Fabp4 and C/EBPα. These findings imply that a decline in endogenous miR-130b-3p or miR-301b-3p is required for iWAT progenitor cells to develop into beige adipocytes but not white adipocytes.

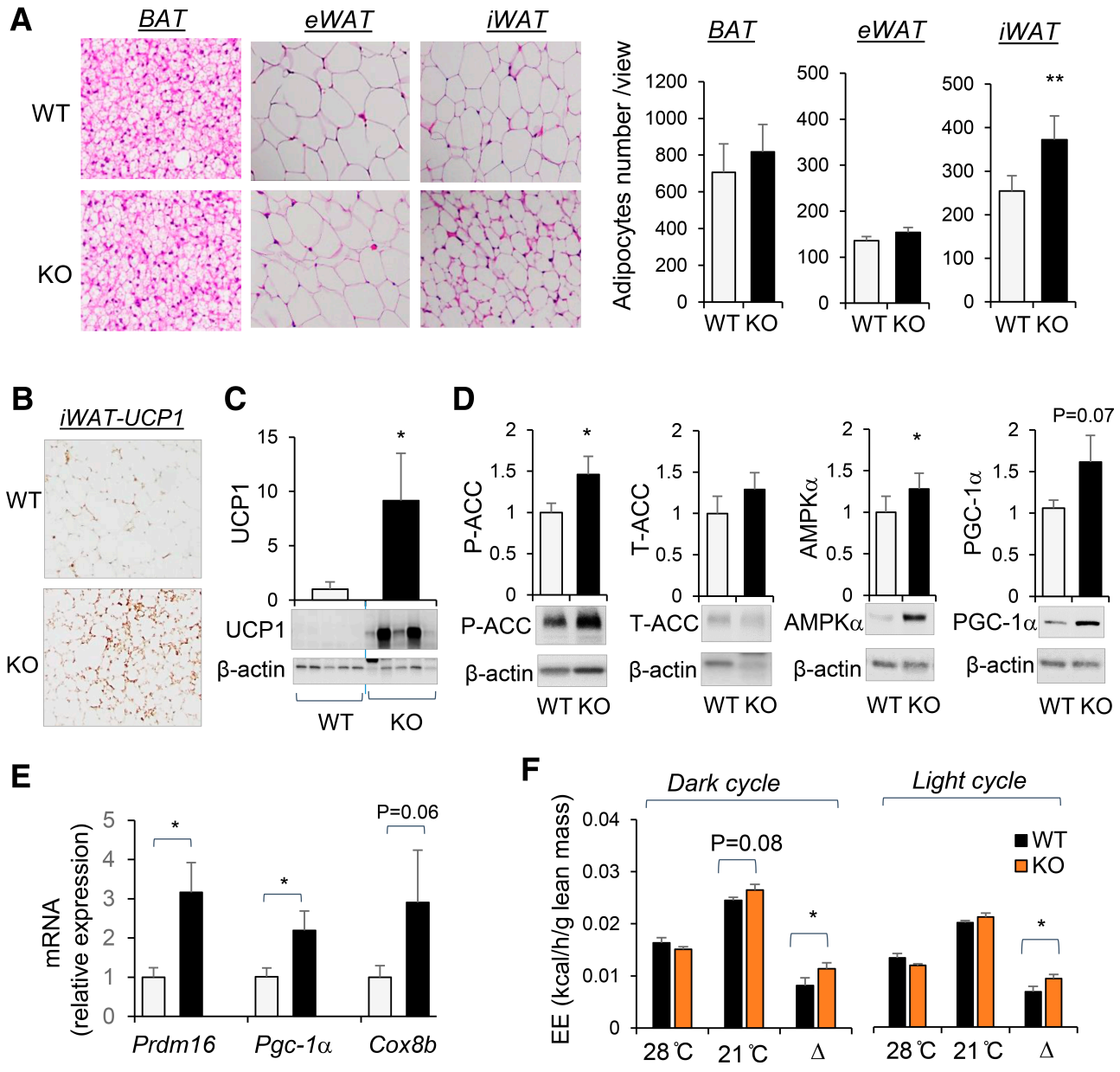

Figure 6—Lack of miR-130b/301b decreased adipocyte size and increased UCP-1 level in iWAT and whole-body EE capacity. miR-130b/301b KO and WT male littermates were fed with HFD (45% kcal from fat, 20% kcal protein, 35% kcal carbohydrate) at 5–6 weeks of age for 12 weeks. *A*: Representative images of hematoxylin-eosin staining of BAT, eWAT, and iWAT in WT and KO groups. Bar graphs show count of cell numbers of BAT, eWAT, and iWAT. *B*: Immunohistochemistry staining of UCP1 in iWAT of WT and KO mice with HFD feeding. *C* and *D*: Proteins were extracted from iWAT tissues and subjected to Western blot analysis with antibodies for UCP-1, P-ACC (S79), total ACC, AMPKα, PGC-1α, and β-actin. Representative blots and quantifications normalized to β-actin are presented. Mean ± SEM, $n = 7$ WT-KO littermate pairs. *E*: Total RNAs were extracted from iWAT tissues, and mRNA expression of *Prdm16*, *Pgc-1α*, and *Cox8b* was measured by real-time PCR and normalized to TBP. Mean ± SEM, $n = 7$ WT-KO littermate pairs. *F*: After HFD for 10 weeks, the mice were placed in a metabolic cage for indirect calorimetry measurement (at 21°C). EE was measured again in the same mice at thermoneutrality (28°C). EE normalized to lean mass at dark (left panel) and light (right panel) cycles measured at 28°C and 21°C and reduced EE (Δ, difference in EE measured at 21°C and 28°C) are presented. Mean ± SEM, $N = 7$ WT-KO littermate pairs. *$P < 0.05$; **$P < 0.01$. T, total.

We propose that the effects of miR-130b/301b on beige adipogenesis are due to direct effects on the expression of AMPKα in adipocyte precursors. AMPK is a central regulator of energy metabolism, including brown fat development and adipogenesis (8,22,35). AMPK activation demethylates Prdm16 promoter (22), increases UCP1 expression, and induces brown/beige adipogenesis in WAT (35,36). In addition, AMPK activation induces expression of PGC-1α, which plays a crucial role in mitochondrial biogenesis and regulating thermogenic gene expression (37). Expression of AMPK is reduced in fat tissue of humans with obesity (38), and miR-130b is known to target the 3′-UTR of AMPKα mRNAs (19–21). Here we confirmed AMPKα1 as the direct target of miR-130b and miR-301b

in iWAT progenitor cells by luciferase reporter assay. We demonstrated regulation of AMPKα and PGC-1α by miR-130b-3p in the context of beige adipogenesis, as overexpression of miR-130b-3p in iWAT progenitor cells decreased the abundance of PGC-1α and AMPKα1 and reduced AMPK activation concomitant with decreased UCP1 abundance. In contrast, lack of miR-130b/301b resulted in increased protein abundance of AMPKα and PGC-1α in iWAT of mice. Thus, we propose that miR-130b/301b plays a critical role in regulating the AMPK/PGC-1α/mitochondrial biogenesis signaling network during beige adipogenesis. Similar to AMPK, PGC-1α is reported to be a direct target of miR-130b-3p (20). PGC-1α expression can be regulated directly by miR-130b, as well as downstream of AMPK. Overexpression of miR-130b-3p in mature beige adipocytes did not impact expression of *Ucp1*, *Cox8a*, or *Pgc-1α*, suggesting that miR-130b more likely acts early on progenitor cells to impact their capacity to differentiate to beige adipocytes and thermogenic function.

Thermogenic respiration by brown and beige adipocytes contributes significantly to whole-body EE and thereby affects fat storage and glucose homeostasis (3,39). We show that mice lacking miR-130b/301b have reduced adiposity and improved glucose tolerance on an HFD. Also, miR-130b/301b deficiency increases expression of UCP-1 in iWAT consistent with activation of thermogenesis. As chronic cold temperature (21°C) triggers an increase in adaptive thermogenesis in mice (40), the net increase in EE between 28°C and 21°C suggests that deletion of miR-130b/301b in mice increased the capacity for thermogenesis and EE in response to cold stimulation. This phenotype aligns with the impaired beige adipocyte differentiation of iWAT progenitors overexpressing miR-130b/301b observed in vitro.

AMPK regulates lipid metabolism through P–acetyl-CoA carboxylase (P-ACC), a bona fide substrate of AMPK (41), which decreases de novo lipogenesis and increases fat oxidation (42). Increased AMPK protein and P-ACC were observed in iWAT of miR-130b/301b KO mice, indicating the activation of AMPK. Along with increased UCP-1 and mRNA expression of *Prdm16*, *Pgc-1α*, and *Cox8b*, those findings explain the smaller iWAT lipid droplets, increased EE, less obesity, and better glucose tolerance in the miR-130b/301b KO mice. Interestingly, smaller adipocyte size and lipid droplets was observed in iWAT but not in BAT or eWAT of miR-130b/301b KO mice. Unlike subcutaneous white fat tissue (iWAT), visceral fat tissue (eWAT) exhibits lower browning capacity (43). As expression of miR-130b is enriched in iWAT, it is plausible that miR-130b/301b plays a unique role in determining beiging within subcutaneous fat. Lack of effect of miR-130b/301b on brown fat may explain in part that whole-body metabolic alteration by miR-130b/301b deletion, such as decreased adiposity, with relatively small impact on overall body weight.

As an miRNA cluster, miR-130b-3p and miR-301b-3p both inhibit beige adipogenesis of iWAT progenitors, and they both target and suppress AMPKα expression. However, different effects of miR-130b-3p and miR-301b-3p on mitochondrial proteins and respiration were observed. The lack of effect of miR-301b on suppressing PGC-1α expression can explain the distinction in effect on mitochondrial maximal respiration. The common and unique mRNA targets of miR-130b and 301b allow them to play regulatory roles in several components of a cellular process within the same pathway to achieve more effective biological function (44).

The strengths of the current study include the assessment of miR-130b/301b function by combined in vivo and in vitro approaches using genetic KO mice and primary progenitors. Results of both approaches are consistent with proposed mechanisms. Given the homology between miR-130b-3p and miR-301b-3p and likelihood of coexpression, removing both from the genome for our studies avoided the potential of one compensating for the other. However, this made dissecting their potential separate roles in vivo difficult. Additional limitations of the current study are that only male mice were studied and other tissues that could be affected by these miRNAs were not examined. As there is a significant amount of miR-130b in extracellular vesicles in circulation (19) the major cell source remains unclear. Thus, specific KO in local adipocytes may not prevent the extracellular uptake of miR-130b/301b. It was therefore necessary to use global KO mice to delete miR-130b/301b systemically and locally to observe the phenotype. Future studies using tissue-specific KO mice targeting the main source of miR-130b/301b and cell-cell interactions are warranted.

In summary, the current study describes a new role of miR-130b/301b in suppressing beige adipogenesis, in EE, and affecting glucose homeostasis, particularly under conditions of HFD. In so doing we have identified miR-130b as a potential link between conditions such as diabetes and obesity where miR-130b expression is increased (13,17, 18,20) and beiging of subcutaneous fat restrained (5,45). miR-130b/301b now join other miRNAs, such as miR194a/214 cluster (46), miR-133a (47), and miR-155 (48), also reported to inhibit beige adipogenesis. Overall, given the relatively high tissue distribution of miR-130b in iWAT, along with an increase in iWAT adipocyte number in miR-130b KO mice, together with reduction in fat mass and no change in BAT, this suggests that miR-130b controls iWAT beige rather than white adipogenesis. As a cluster of miRNAs dysregulated in metabolic diseases, miR-130b/301b is therefore a potential therapeutic target to counter against obesity and associated disorders.

Funding. This study is supported by Oklahoma Center for the Advancement of Science and Technology (OCAST) (principle investigator: S.J.) and Oklahoma IDeA Network of Biomedical Research Excellence (OK-INBRE) (principle

investigator: S.J.) grants and the CMRI Metabolic Research Program in section of Pediatric Endocrinology and Diabetes, University of Oklahoma. This publication was made possible by National Institutes of Health grant 5P30GM122744 from the Centers of Biomedical Research Excellence (COBRE) program of the National Institute of General Medical Sciences. The Seahorse XFe96 equipment provided by the Cancer Functional Genomics core (Stephenson Cancer Center, University of Oklahoma) was supported partly by National Institute of General Medical Sciences grant P20GM103639 and National Cancer Institute grant P30CA225520 of the National Institutes of Health.

Duality of Interest. No potential conflicts of interest relevant to this article were reported.

Author Contributions. All authors contributed to the study conception and design and interpretation of data. W.L., Y.K., M.E.J., O.H.-P., and S.J. performed the experiments. J.E.F., S.D.C., and S.J. wrote the manuscript. All authors revised the manuscript and approved this version to be published. S.J. is the guarantor of this work and, as such, had full access to all the data in the study and takes responsibility for the integrity of the data and the accuracy of the data analysis.

Prior Presentation. Parts of this study were presented in abstract form at the virtual Keystone Symposia on Obesity, 1 February 2021.

References

1. Spiegelman BM, Flier JS. Obesity and the regulation of energy balance. Cell 2001;104:531–543

2. Cypess AM, Kahn CR. The role and importance of brown adipose tissue in energy homeostasis. Curr Opin Pediatr 2010;22:478–484

3. Sidossis L, Kajimura S. Brown and beige fat in humans: thermogenic adipocytes that control energy and glucose homeostasis. J Clin Invest 2015;125:478–486

4. Ohtomo T, Ino K, Miyashita R, et al. Chronic high-fat feeding impairs adaptive induction of mitochondrial fatty acid combustion-associated proteins in brown adipose tissue of mice. Biochem Biophys Rep 2017;10:32–38

5. Alcalá M, Calderon-Dominguez M, Serra D, Herrero L, Viana M. Mechanisms of impaired brown adipose tissue recruitment in obesity. Front Physiol 2019;10:94

6. Shao M, Ishibashi J, Kusminski CM, et al. Zfp423 maintains white adipocyte identity through suppression of the beige cell thermogenic gene program. Cell Metab 2016;23:1167–1184

7. Lidell ME, Betz MJ, Dahlqvist Leinhard O, et al. Evidence for two types of brown adipose tissue in humans. Nat Med 2013;19:631–634

8. Ahmad B, Serpell CJ, Fong IL, Wong EH. Molecular mechanisms of adipogenesis: the anti-adipogenic role of AMP-activated protein kinase. Front Mol Biosci 2020;7:76

9. Van Nguyen TT, Vu VV, Pham PV. Transcriptional factors of thermogenic adipocyte development and generation of brown and beige adipocytes from stem cells. Stem Cell Rev Rep 2020;16:876–892

10. Karbiener M, Scheideler M. MicroRNA functions in Brite/brown fat - novel Perspectives towards Anti-Obesity Strategies. Comput Struct Biotechnol J 2014;11:101–105

11. Bartel DP. MicroRNAs: genomics, biogenesis, mechanism, and function. Cell 2004;116:281–297

12. Ivey KN, Srivastava D. MicroRNAs as regulators of differentiation and cell fate decisions. Cell Stem Cell 2010;7:36–41

13. Wagschal A, Najafi-Shoushtari SH, Wang L, et al. Genome-wide identification of microRNAs regulating cholesterol and triglyceride homeostasis. Nat Med 2015;21:1290–1297

14. Zhao H, Shen J, Daniel-MacDougall C, Wu X, Chow WH. Plasma MicroRNA signature predicting weight gain among Mexican-American women. Obesity (Silver Spring) 2017;25:958–964

15. Hirono T, Jingushi K, Nagata T, et al. MicroRNA-130b functions as an oncomiRNA in non-small cell lung cancer by targeting tissue inhibitor of metalloproteinase-2. Sci Rep 2019;9:6956

16. Fort RS, Mathó C, Oliveira-Rizzo C, Garat B, Sotelo-Silveira JR, Duhagon MA. An integrated view of the role of miR-130b/301b miRNA cluster in prostate cancer. Exp Hematol Oncol 2018;7:10

17. Tryggestad JB, Teague AM, Sparling DP, Jiang S, Chernausek SD. Macrophage-derived microRNA-155 increases in obesity and influences adipocyte metabolism by targeting peroxisome proliferator-activated receptor gamma. Obesity (Silver Spring) 2019;27:1856–1864

18. Tryggestad JB, Vishwanath A, Jiang S, et al. Influence of gestational diabetes mellitus on human umbilical vein endothelial cell miRNA. Clin Sci (Lond) 2016;130:1955–1967

19. Gan L, Xie D, Liu J, et al. Small extracellular microvesicles mediated pathological communications between dysfunctional adipocytes and cardiomyocytes as a novel mechanism exacerbating ischemia/reperfusion injury in diabetic mice. Circulation 2020;141:968–983

20. Wang YC, Li Y, Wang XY, et al. Circulating miR-130b mediates metabolic crosstalk between fat and muscle in overweight/obesity. Diabetologia 2013;56:2275–2285

21. Chen Z, Luo J, Ma L, et al. MiR130b-regulation of PPARγ coactivator- 1α suppresses fat metabolism in goat mammary epithelial cells. PLoS One 2015;10:e0142809

22. Yang Q, Liang X, Sun X, et al. AMPK/α-ketoglutarate axis dynamically mediates DNA demethylation in the Prdm16 promoter and brown adipogenesis. Cell Metab 2016;24:542–554

23. Wu L, Zhang L, Li B, et al. AMP-activated protein kinase (AMPK) regulates energy metabolism through modulating thermogenesis in adipose tissue. Front Physiol 2018;9:122

24. Zhao J, Yang Q, Zhang L, et al. AMPKα1 deficiency suppresses brown adipogenesis in favor of fibrogenesis during brown adipose tissue development. Biochem Biophys Res Commun 2017;491:508–514

25. Schwenk F, Baron U, Rajewsky K. A cre-transgenic mouse strain for the ubiquitous deletion of loxP-flanked gene segments including deletion in germ cells. Nucleic Acids Res 1995;23:5080–5081

26. Hong J, Stubbins RE, Smith RR, Harvey AE, Núñez NP. Differential susceptibility to obesity between male, female and ovariectomized female mice. Nutr J 2009;8:11

27. Morris EM, Noland RD, Allen JA, et al. Difference in housing temperature-induced energy expenditure elicits sex-specific diet-induced metabolic adaptations in mice. Obesity (Silver Spring) 2020;28:1922–1931

28. Kilroy G, Dietrich M, Wu X, Gimble JM, Floyd ZE. Isolation of Murine Adipose-Derived Stromal/Stem Cells for Adipogenic Differentiation or Flow Cytometry-Based Analysis. Methods Mol Biol 2018;1773:137–146

29. Trajkovski M, Ahmed K, Esau CC, Stoffel M. MyomiR-133 regulates brown fat differentiation through Prdm16. Nat Cell Biol 2012;14:1330–1335

30. Suwandhi L, Altun I, Karlina R, et al. Asc-1 regulates white versus beige adipocyte fate in a subcutaneous stromal cell population. Nat Commun 2021;12:1588

31. de Jesus LA, Carvalho SD, Ribeiro MO, et al. The type 2 iodothyronine deiodinase is essential for adaptive thermogenesis in brown adipose tissue. J Clin Invest 2001;108:1379–1385

32. Virtue S, Vidal-Puig A. Assessment of brown adipose tissue function. Front Physiol 2013;4:128

33. Zoico E, Rubele S, De Caro A, et al. Brown and beige adipose tissue and aging. Front Endocrinol (Lausanne) 2019;10:368

34. Ong FJ, Ahmed BA, Oreskovich SM, et al. Recent advances in the detection of brown adipose tissue in adult humans: a review. Clin Sci (Lond) 2018;132:1039–1054

35. Desjardins EM, Steinberg GR. Emerging role of AMPK in brown and beige adipose tissue (BAT): implications for obesity, insulin resistance, and type 2 diabetes. Curr Diab Rep 2018;18:80

36. Vila-Bedmar R, Lorenzo M, Fernández-Veledo S. Adenosine 5′-monophosphate-activated protein kinase-mammalian target of rapamycin cross talk regulates brown adipocyte differentiation. Endocrinology 2010;151:980–992

37. Gill JA, La Merrill MA. An emerging role for epigenetic regulation of Pgc-1α expression in environmentally stimulated brown adipose thermogenesis. Environ Epigenet 2017;3:dvx009
38. Xu XJ, Gauthier MS, Hess DT, et al. Insulin sensitive and resistant obesity in humans: AMPK activity, oxidative stress, and depot-specific changes in gene expression in adipose tissue. J Lipid Res 2012;53:792–801
39. Wang W, Seale P. Control of brown and beige fat development. Nat Rev Mol Cell Biol 2016;17:691–702
40. Bastías-Pérez M, Zagmutt S, Soler-Vázquez MC, Serra D, Mera P, Herrero L. Impact of adaptive thermogenesis in mice on the treatment of obesity. Cells 2020;9:316
41. Lepropre S, Kautbally S, Octave M, et al. AMPK-ACC signaling modulates platelet phospholipids and potentiates thrombus formation. Blood 2018;132: 1180–1192
42. Bijland S, Mancini SJ, Salt IP. Role of AMP-activated protein kinase in adipose tissue metabolism and inflammation. Clin Sci (Lond) 2013;124:491–507
43. Cohen P, Levy JD, Zhang Y, et al. Ablation of PRDM16 and beige adipose causes metabolic dysfunction and a subcutaneous to visceral fat switch. Cell 2014;156:304–316
44. Altuvia Y, Landgraf P, Lithwick G, et al. Clustering and conservation patterns of human microRNAs. Nucleic Acids Res 2005;33:2697–2706
45. Sakamoto T, Nitta T, Maruno K, et al. Macrophage infiltration into obese adipose tissues suppresses the induction of UCP1 level in mice. Am J Physiol Endocrinol Metab 2016;310:E676–E687
46. He L, Tang M, Xiao T, et al. Obesity-associated miR-199a/214 cluster inhibits adipose browning via PRDM16-PGC-1α transcriptional network. Diabetes 2018;67:2585–2600
47. Liu W, Bi P, Shan T, et al. miR-133a regulates adipocyte browning in vivo. PLoS Genet 2013;9:e1003626
48. Chen Y, Siegel F, Kipschull S, et al. miR-155 regulates differentiation of brown and beige adipocytes via a bistable circuit. Nat Commun 2013; 4:1769